11. Crystal data for **1**: cubic, space group $I\bar{4}3m$ (#217), a = 15.0487(18) Å at −140°C and R factor (weighted R) = 0.026(0.031).
12. Considering the protrusion of the molybdenyl groups into the cubic cavities, the size of the cavities can be estimated as follows. One can obtain a maximum value by taking the cube root of the volume of the cavity obtained from the defect analogy of **1** and NbO (see text), which yields a value of $[0.25(3408)]^{0.33}$ = 9.5 Å. Alternatively, one can derive a minimum value by subtracting the appropriate bond lengths from the unit cell edge: two times the molybdenyl Mo–O distance plus two times the Mo–O trans to the molybdenyl group plus one oxygen diameter, which gives 1.6 + 2.4 + 2.8 = 6.8 Å, but this estimate does not include the volume in the "corners" of the cubic cavities between the protruding molybdenyl groups.
13. A. L. Bowman, *Acta Crystallogr.* **21**, 843 (1966).
14. Because the total amount of organic cation present as determined from the x-ray data was in agreement with the results of the elemental analysis, we used the N:Mo ratio from the x-ray analysis to determine the calculated empirical formula of **1**: calculated for anhydrous $[(Me_4N)_{1.33}(H)_{0.67}][Mo_4P_2O_{16}]$: C, 7.98%; H, 2.12%; N, 2.32%; P, 7.74%; and Mo, 47.97%; found: C, 8.50%; H, 2.51%, N, 2.31%; P, 7.43%; and Mo, 47.30%.
15. D. M. Ruthven, *Principles of Adsorption and Adsorption Processes* (Wiley, New York, 1984), p. 49.
16. D. W. Breck, *Zeolite Molecular Sieves* (Wiley-Interscience, New York, 1974), p. 636.
17. E. W. Corcoran, Jr., unpublished results; R. C. Haushalter and L. Mundi, unpublished results.
18. Chem-X, Chemical Design, Ltd., Mahwah, NJ.
19. We are grateful to H. G. von Schnering for pointing out several important features of the structure, for noting the similarity between the vacancy ordering in this structure and that of NbO, and for many useful discussions.

6 July 1989; accepted 2 October 1989

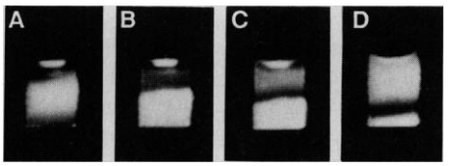

Fig. 1. Light scattering of oscillating microtubules. The reaction was started by filling 200 μl of the cold protein solution in a cuvette thermostatted at 37°C; the images were taken (**A**) 532, (**B**) 555, (**C**) 605, and (**D**) 655 s after the temperature jump. The light scattering indicates microtubule assembly. An assembly wave moves from top to bottom at about 0.015 mm/s. The width of the cell is 4 mm. Tubulin was purified from porcine brain as described (*6*). Oscillations were obtained at high protein concentrations (typically 10 to 50 mg/ml) in various buffer conditions, for example 0.1*M* Pipes (1,4-piperazinediethanesulfonic acid), *p*H 6.9, 20 m*M* $MgSO_4$, 60 m*M* NaCl, 1 m*M* EGTA, 1m*M* dithiothreitol, and 6 m*M* GTP.

Spatial Patterns from Oscillating Microtubules

ECKHARD MANDELKOW, EVA-MARIA MANDELKOW, HIROKAZU HOTANI, BENNO HESS, STEFAN C. MÜLLER

Microtubules are fibers of the cytoskeleton involved in the generation of cell shape and motility. They can be highly dynamic and are capable of temporal oscillations in their state of assembly. Solutions of tubulin (the subunit protein of microtubules) and guanosine triphosphate (GTP, the cofactor required for microtubule assembly and oscillations) can generate various dissipative structures. They include traveling waves of microtubule assembly and disassembly as well as polygonal networks. The results imply that cytoskeletal proteins can form dynamic spatial structures by themselves, even in the absence of cellular organizing centers. Thus the microtubule system could serve as a simple model for studying pattern formation by biomolecules in vitro.

THE SELF-ASSEMBLY OF BIOPOLYmers from their subunits is usually described in terms of the helical condensation theory (*1*). The model contains the phases of nucleation, followed by elongation of subunits onto the polymer ends until a steady state of assembly is attained. The model also assumes a homogeneous distribution of all reacting species. In the case of microtubules, the simple condensation model was superseded by that of dynamic instability (*2*), where—even at steady state—some polymers grow while others shrink. Microtubules are the only biopolymers known that exhibit this unusual behavior; it depends on the hydrolysis of GTP that accompanies microtubule assembly. One can even synchronize an entire population of microtubules so that they grow or shrink simultaneously; this leads to oscillations in the level of assembly that can be observed by light or x-ray scattering (*3–6*). The mechanism of oscillations proposed previously (*5, 6*) contains the following steps. Microtubules are formed from their subunits tubulin (Tu) with bound GTP (Tu·GTP); GTP is hydrolyzed during assembly, leading to the destabilization of microtubules; microtubules depolymerize into tubulin oligomers which contain bound GDP (guanosine diphosphate); oligomers dissociate into tubulin with bound GDP (Tu·GTP); and GDP is replaced by GTP from the solution so that assembly-competent Tu·GTP is regenerated. Since the dissolution of oligomers is slow they can be regarded as a "refractory" state. The transition from microtubule growth to shrinkage can be modeled by cooperativity between tubulin subunits on microtubule ends. Computer simulations show that this model can explain the observed homogeneous oscillations, but it does not predict spatial patterns.

Whereas previous reports (*3–6*) have dealt with the case of spatially homogeneous oscillations, we now give an example of an inhomogeneous oscillation generating a simple spatial pattern (Fig. 1). A cold tubulin solution (0°C) was filled into a cuvette thermostatted at 37°C. After a lag of about 30 s, microtubules assemble and oscillate with a periodicity of 210 s. However, different parts of the solution oscillate with a shift in phase so that waves of assembly and disassembly appear to be rolling from the top to the bottom of the tube. This behavior is not due to a gradient in temperature because this equilibrates within a few seconds, well before the onset of assembly.

More detailed information can be obtained by a two-dimensional ultraviolet (UV) spectrophotometer designed to study the Belousov-Zhabotinskii (BZ) reaction (*7*). In Fig. 2 results are shown for an experiment in which the cold protein solution was filled into a thermostatted petri dish so that the final temperature of about 37°C was reached within a few seconds. The reaction started after a lag time of about 30 s; it was observed by the transmitted intensity of a parallel beam of UV light (390 nm) recorded on a TV detector. One observes concentric rings of high scattering (green to light blue in the color coding of Fig. 2, A through C) typically a few millimeters wide, originating at the periphery and traveling toward the center where they disappear. As in Fig. 1, the scattering is due to microtubule assembly; the periodicity of the waves is of the same order as that of the homogeneous microtubule oscillations described previously, that is, about 1 to 3 min, depending on buffer conditions. Similar observations can be made in reflected light by time-lapse cinematography (Fig. 2, D through F), except that the contrast is reversed. During an experiment the frequency of wave generation at the periphery remains roughly constant, but the speed of propagation toward the center tends to decrease. As a result the number of visible wave crests increases with time (Fig. 2, A through C).

The patterns described above are easily seen by eye, but there are two other types of patterns visible only a higher resolution in

E. Mandelkow and E.-M. Mandelkow, Max-Planck-Unit for Structural Molecular Biology, c/o DESY, Notkestrasse 85, D-2000 Hamburg 52, West Germany.
H. Hotani, ERATO, Molecular Dynamic Assembly Project, 15 Morimoto-cho, Shimogamo, Kyoto 606, Japan.
B. Hess and S. C. Müller, Max-Planck-Institut für Ernährungsphysiologie, Rheinlanddamm 201, D-4600 Dortmund 1, West Germany.

the UV spectrophotometer (Fig. 3). They are two sets of polygons, typically 0.5 to 1 mm in size. Shortly before the arrival of a microtubule-assembly wave, a network of polygons outlined with sharp bright edges appears first (Fig. 3A). This assembly is followed by another network, bounded by dark edges that are often perpendicular to the first set of edges. Thus the two networks appear to be interlaced. Both networks become invisible when the microtubule assembly wave travels through (dark, approaching from top in Fig. 3A), and the first network reappears afterwards, but with reversed contrast (that is, now with dark edges). The polygons can be identified because they remain stationary. It seems that the solution initially develops a substructure that it "remembers" at later times independently of the assembly cycles. A pseudocolor enhanced image of the network is shown in Fig. 3B (red and yellow, with a microtubule assembly wave approaching in blue). Similar polygonal networks have been described in other oscillating systems such as the glycolysis in yeast extracts (*8*) or the BZ reaction (*9*). The interpretation in our case is not clear at present. One possibility is that they are due to hydrodynamic instabilities. The correlation with the onset of microtubule assembly suggests that the change in viscosity may play an important role; in other words, the chemical reaction itself could influence the pattern [see (*10*)].

A view of the small-scale inhomogeneities in an oscillating solution can be obtained by dark-field video microscopy [Fig. 4; for methods, see (*11*)]. In this case the field of view is less than 0.1 mm, much smaller than the dimensions of the traveling waves or the polygons so that the formation and propagation of these patterns cannot be observed. Instead one sees the local buildup and destruction of microtubules. At the onset of assembly one observes first many short bright filaments (Fig. 4A) that gradually grow and form a dense network (Fig. 4B). The denser the network, the more the Brownian motion of background particles becomes inhibited, indicating an increase in viscosity. During the disassembly phase many of the microtubules vanish (Fig. 4C); they regrow later during the next assembly wave (Fig. 4D). A notable feature is that microtubules have a strong tendency to coalesce into bundles (recognizable by their higher contrast and stiffness), even at early stages of assembly. Although most bundles disappear during the disassembly phase, the thicker ones only shrink in diameter; they become more flexible but do survive, suggesting that microtubules are lost from the periphery of the bundle. Thus a loose network of bundles tends to persist through the minimum of overall assembly (depending on the amplitude of the oscillations, see Fig. 4C) and reassembly appears to start preferentially at these bundles. The apparent spacing between the bundles is typically about 10 to 30 μm. This is about 10- to 100-fold smaller than the dimensions of the polygons described above, indicating that these do not correspond directly to microtubule bundles. However, the persistence of some bundles might explain why the solution "remembers" the positions of the polygons from one assembly cycle to the next.

The oscillating spatial patterns described here have different aspects in different spatial dimensions, separated by one or more orders of magnitude: macroscopic linear or concentric waves (typically in the 5-mm range; Figs. 1 and 2), intermediate ripples and polygons (around 0.5 to 1 mm; Fig. 3), and microscopic microtubules and microtubule bundles (spaced typically 10 μm apart; Fig. 4). The microscopic aspect is best described in terms of a network that is periodi-

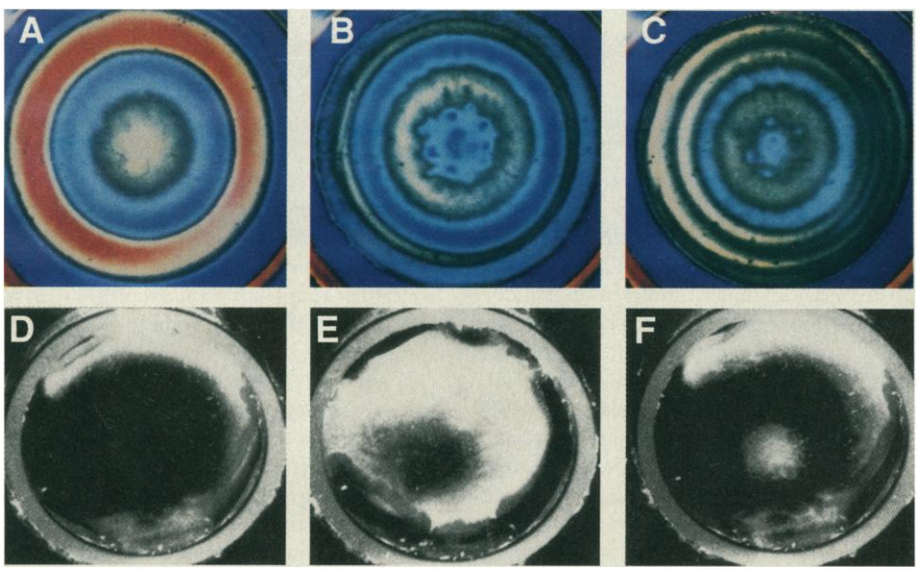

Fig. 2. (**A** to **C**) Spatial patterns of oscillating microtubules in a thin layer of tubulin solution [contained within a sealing ring of 22-mm inner diameter (dark blue), filled with 200 μl of protein solution, 46 mg/ml] and observed in transmission mode by a two-dimensional UV spectrophotometer at 390 nm (*7*). The maxima of turbidity (pseudocolor green to light blue) correspond to maxima in microtubule assembly; they are separated by regions of assembly minima (red to yellow). The images were taken 182, 499, and 949 s after the temperature jump (from left to right). (A) The first wave crest has moved halfway toward the center, the second is just forming at the periphery. (B) The crests of the second, third, and fourth waves are seen simultaneously; the second has just reached the center (note the small-scale inhomogeneities), and the fourth is forming at the periphery. (C) Crests of waves 4 (center) to 7 are visible. (**D** to **F**) Similar set of experiments observed in reflection mode by illumination from above and recording on 16-mm film (400 μl of protein solution, 59 mg/ml). The sealing ring and the microtubule assembly maxima appear bright. The first wave appears at the periphery (D), moves inwards (E), and disappears at the center (F). The second wave forms at the periphery (F) with roughly the same spatial distribution as the first. Note that the wavelength is longer than in (A through C) and that the waves are not circularly symmetric.

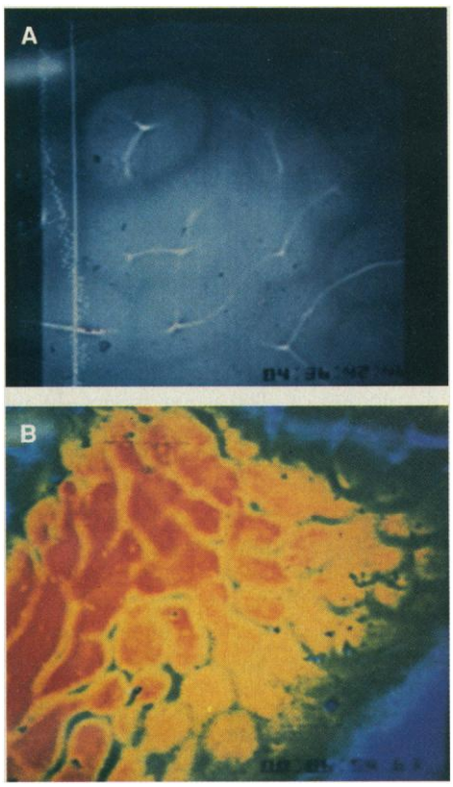

Fig. 3. Networks of polygons observed with the UV spectrophotometer (**A**) without and (**B**) with pseudocoloring of the scattering intensity. The bright and dark edges are best seen in (A). In both cases the network is recorded shortly before the arrival of the microtubule assembly wave [dark in the outer area of (A), and blue in (B)]. The width of the area is 5 mm.

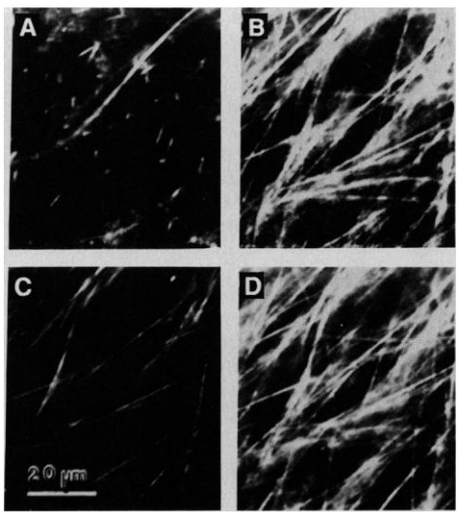

Fig. 4. Oscillating microtubules seen by dark-field video microscopy (*11*). (**A**) Beginning of the first assembly phase (135 s after the temperature shift). Note the numerous short rods; because of their high contrast they probably correspond to short microtubule bundles. (**B**) Maximum of first assembly (t = 258 s). Note the dense meshwork of microtubules (mostly bundles) and the high background (containing additional single microtubules which have a weak contrast and are not resolved). (**C**) Assembly minimum following the first maximum (t = 403 s). Note the decrease in the microtubule density and the lower background. A fraction of microtubule bundles remains through the disassembly phase. (**D**) Second assembly maximum (t = 482 s). Note that some of the prominent bundles retain their relative positions during the cycles.

cally built up and destroyed. Some of the stabler elements (for example, microtubule bundles) may persist through the oscillations and change only in apparent width, contrast, and flexibility. These elements remain nearly stationary. The intermediate-range polygons could correspond to hydrodynamic instabilities caused, for example, by the Marangoni effect. In the present case the viscosity is strongly modulated by microtubule assembly, so that the pattern of convection cells may in turn depend on the pattern of microtubules. The polygons also seem to be stationary in space, that is, when they are visible (just before or after a wave) they appear at the same positions. On the macroscopic levels the spatial patterns are dominated by the traveling waves of microtubule assembly. They broadly resemble the trigger waves of the BZ reaction. These have been explained by three conditions [reviewed in (*12*)]: (i) the solution must be in an excitable state; (ii) the reaction is started at a nucleation site and then proceeds autocatalytically by diffusion coupling; and (iii) waves occur because the initial reaction is followed by a transient refractory state. Analogous arguments can be applied to the present case: (i) The solution is initially in an excitable state because tubulin is ready to polymerize at 37°C; (ii) in the case of a circular layer of solution the nucleation barrier appears to be lowest at the periphery; and (iii) the refractory state (following microtubule disassembly) is dominated by tubulin oligomers that transiently trap the protein in an assembly-incompetent form (*5*).

What conclusions can one draw for pattern formation in living cells? Microtubules are known to be important for their shape and motility, but the mechanism and the interactions with other cellular elements are not well understood. Thus the mechanisms that generate the spatial patterns of living cells are difficult to explain in molecular terms. The point to be learned from the present results is that microtubules alone are capable of organizing themselves in time and space. The patterns we observe are simple, and moreover they are generated from only two types of molecules, tubulin and GTP. This simplicity opens the way of studying the mechanisms underlying microtubule self-organization that could lead to a better understanding of cellular pattern formation.

REFERENCES AND NOTES

1. F. Oosawa and S. Asakura, *Thermodynamics of the Polymerization of Protein* (Academic Press, London, 1975).
2. T. Mitchison and M. Kirschner, *Nature* **312**, 237 (1984).
3. M. F. Carlier, R. Melki, D. Pantaloni, T. L. Hill, Y. Chen, *Proc. Natl. Acad. Sci. U.S.A.* **84**, 5257 (1987).
4. F. Pirollet, D. Job, R. L. Margolis, J. R. Garel, *EMBO J.* **6**, 3247 (1987).
5. E.-M. Mandelkow, G. Lange, A. Jagla, U. Spann, E. Mandelkow, *ibid.* **7**, 357 (1988).
6. G. Lange, E.-M. Mandelkow, A. Jagla, E. Mandelkow, *Eur. J. Biochem.* **178**, 61 (1988).
7. S. C. Müller, T. Plesser, B. Hess, *Science* **230**, 661 (1985).
8. S. C. Müller, T. Plesser, A. Boiteux, B. Hess, *Z. Naturforsch.* **40c**, 588 (1985).
9. A. M. Zhabotinskii and A. N. Zaikin, *J. Theor. Biol.* **40**, 45 (1973).
10. D. Avnir and M. Kagan, *Nature* **307**, 717 (1984).
11. T. Horio and H. Hotani, *ibid* **321**, 605 (1986).
12. J. Ross, S. C. Müller, C. Vidal, *Science* **240**, 460 (1988).

13. We thank P. Derr for technical assistance in the protein preparation, and T. Freundner for his help in producing movie sequences of oscillating microtubule solutions. Supported by the Bundesministerium für Forschung und Technologie. Readers interested in obtaining video or film sequences of experiments described here should write to the first author.

21 July 1989; accepted 25 September 1989

A Formalin-Inactivated Whole SIV Vaccine Confers Protection in Macaques

MICHAEL MURPHEY-CORB,* LOUIS N. MARTIN, BILLIE DAVISON-FAIRBURN, RONALD C. MONTELARO, MARK MILLER, MELANIE WEST, SUSUMU OHKAWA, GARY B. BASKIN, JING-YU ZHANG, SCOTT D. PUTNEY, ANTHONY C. ALLISON, DEBORAH A. EPPSTEIN

A vaccine against human immunodeficiency virus (HIV) would be highly effective in stopping the acquired immunodeficiency syndrome (AIDS) epidemic. A comprehensive evaluation of potential vaccine methodologies can be made by means of the simian model for AIDS, which takes advantage of the similarities in viral composition and disease potential between simian immunodeficiency virus (SIV) infection of rhesus macaques and HIV infection in humans. Immunization with a formalin-inactivated whole SIV vaccine potentiated with either alum and the Syntex adjuvant threonyl muramyl dipeptide (MDP) or MDP alone resulted in the protection of eight of nine rhesus monkeys challenged with ten animal-infectious doses of pathogenic virus. These results demonstrate that a whole virus vaccine is highly effective in inducing immune responses that can protect against lentivirus infection and AIDS-like disease.

DEVELOPMENT OF A VACCINE FOR HIV, the causative agent of AIDS, is the most effective means of combating this lethal disease. Since many viral vaccines do not actually prevent initial infection, but act by limiting virus dissemination and establishment after infection (*1–4*), evaluation of the efficacy of a vaccine for HIV solely on the basis of preventing infection may be limiting and misleading. The development of an HIV vaccine for the prevention of AIDS is greatly facilitated by the availability of a nonhuman primate model, the rhesus macaque (*Macaca mulatta*), in

M. Murphey-Corb, L. N. Martin, B. Davison-Fairburn, S. Ohkawa, G. B. Baskin, J.-Y. Zhang, Delta Regional Primate Research Center, Tulane University, Covington, LA 70434.
R. C. Montelaro, M. Miller, M. West, Louisiana State University, Baton Rouge, LA 70803.
S. D. Putney, Repligen Corp., Cambridge, MA 02139.
A. C. Allison and D. A. Eppstein, Syntex Research, Palo Alto, CA 94304.

*To whom correspondence should be addressed.